A PRECISE DETERMINATION OF THE τ-MASS

W. BARTEL, P. DITTMANN, P. DUINKER [1], J. OLSSON, L. O'NEILL, D. PANDOULAS [2] and P. STEFFEN
Deutsches Elektronen-Synchrotron DESY, Hamburg, Germany

and

U. FRITSCHER, J. HEINTZE, G. HEINZELMANN, R.D. HEUER, H. RIESEBERG and A. WAGNER
Physikalisches Institut der Universität Heidelberg, Germany

Received 30 May 1978

The energy dependence of the cross sections for $e^+e^- \to e^\pm(\mu^\pm) + 1$ charged track has been measured for centre of mass energies between 3.60 and 4.40 GeV. The pair production of the τ-lepton is observed at all energies and the τ-mass is determined to be $1.787^{+0.010}_{-0.018}$ GeV from a fit to the energy dependence of the cross section.

Following the discovery of anomalous e–μ events at SPEAR by the SLAC–LBL group [1] substantial evidence for the existence of the heavy lepton τ has been collected by several groups [2,3]. Until now the properties of the τ-lepton have been studied mainly in two types of reactions:

$$e^+e^- \to e^\pm + \mu^\mp + \text{missing energy}, \quad (1)$$

and

$$e^+e^- \to \begin{matrix} e^\pm \\ \mu^\pm \end{matrix} + 1 \text{ charged track} + \begin{matrix} \text{missing energy} \\ \geqslant 0 \text{ photon}. \end{matrix} \quad (2)$$

Reaction (1) has yielded clean samples of τ-pair-production events but with low statistical precision. Reaction (2) on the other hand has yielded samples with better statistics, but with higher background contamination.

In our experiment at the DORIS storage rings at DESY we have investigated the reaction

$$e^+e^- \to \begin{matrix} e^\pm \\ \mu^\pm \end{matrix} + 1 \text{ charged track} + 0 \text{ photon} + \text{missing energy}, \quad (3)$$

which is similar to reaction (2), except that we can and do exclude events in which photons are observed within 96% of the full solid angle.

Final states of one lepton, one charged track of any type, and missing energy carried away by neutrinos can originate from the reaction

$$e^+ + e^- \to \tau^+ + \tau^-, \quad (4)$$

with the subsequent τ-decays: $\tau \to e\nu\nu$, $\mu\nu\nu$, $\pi\nu$, $K\nu$.

The apparatus, of which fig. 1 shows a section transverse to the beam axis, is generally similar to the one which has been described in a previous publication [4]. The inner detector (ID) features three concentric cylindrical drift chambers (CD) for measuring the directions of charged particles, and two concentric, polygonal hodoscopes (H) of scintillation counters for triggering purposes. This inner detector covers the range 30° to 150° in polar scattering angle, or 86% of the full solid sphere, which is also the solid angle for triggering. The solid angle for detecting particles is extended to 96% of 4π sr, by scintillator hodoscopes

[1] Now at NIKHEF, Amsterdam, Netherlands.
[2] Now at Imperial College, London, England.

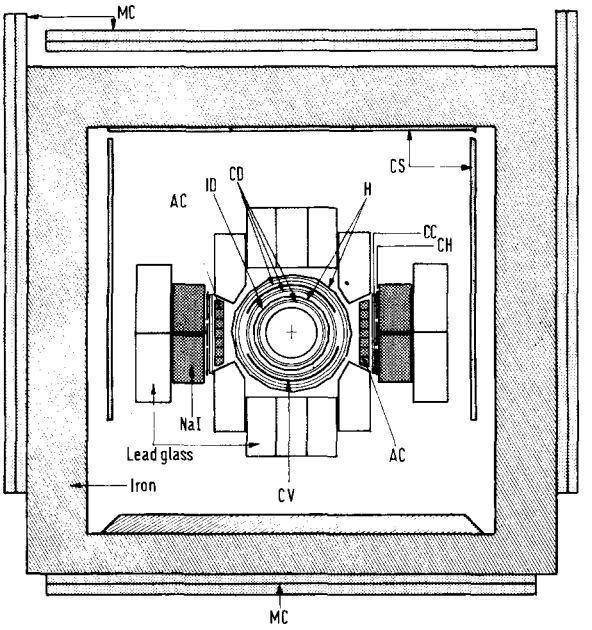

Fig. 1. Experimental apparatus.

(not shown in fig. 1) situated close to the beam pipe and covering the regions of polar angle close to zero and 180 degrees. These hodoscopes are covered with lead in order to convert gamma rays. The very large solid angle for particle recognition is a unique feature of this apparatus and an important advantage for the analysis presented here.

A one radiation length lead converter (CV) covers three quarters of the full azimuthal angle and is situated between the middle and outer drift chambers. The one quarter of the full azimuthal angle corresponding to the gaps in the lead converter is covered by two 1.8 radiation length, segmented, "active" converters (AC) of sodium iodide scintillator, which are situated behind the outermost cylindrical drift chamber. These counter arrays convert gamma rays with high efficiency without loss of energy resolution, since the energy left in the converter is measured. Planar drift chambers (CC) for locating gamma ray conversions, and plastic scintillation counters (CH) for triggering purposes are situated behind the active converters. Behind these latter scintillation counters are "sidewall" arrays of sodium iodide and lead glass energy absorption counters for measuring electron and gamma ray energies with good resolution. Each side wall, together with the adjacent active converter, presents a thickness of 16.2 radiation lengths to particles at normal incidence. Above and below the inner detector lead glass blocks of approximately 12.7 radiation lengths thickness are used for electron and photon detection. The scintillation counters (CS) located above and to both sides of the energy counter arrays are used in rejecting cosmic ray background by time-of-flight techniques. The time-of-flight counters are surrounded by an iron hadron absorber of thirty centimeters thickness, which provides an energy threshold of about 600 MeV for detecting muons. The iron and the energy counters together present 4.6 collision lengths to hadrons. Drift chambers (MC) with fifteen centimeter drift spaces surround the iron absorber. These detect muons over 55% of the full solid sphere.

The triggering criteria for the apparatus consist of various combinations of charged track multiplicity in the inner detector and a minimum total energy registered in the sodium iodide and lead glass counters. In addition, there is a "neutral trigger", which requires no charged track, but at least one gamma ray conversion and at least one GeV measured in the energy counters.

In the analysis presented here, the energy resolution for electromagnetic showers is approximately $13\%/\sqrt{E}$ (FWHM), where "E" is the energy in GeV, in all parts of the apparatus. The angular resolutions for various particle types and components of the apparatus are listed in table 1.

Table 1
Solid angle coverage and angular resolution of apparatus components.

Apparatus component and solid angle	Angular resolution (FWHM)	
Inner detector 86% of 4π	Charged tracks	$\delta\phi$ = 4 mrad $\delta\theta$ = 30 mrad
Active converter and sidewall counters 19% of 4π	Converted photons	$\delta\phi$ = 70 mrad $\delta\theta$ = 80 mrad
Top–bottom lead glass counters 67% of 4π	Converted photons	$\delta\phi$ = 75 mrad $\delta\theta$ = 65 mrad
Muon chambers 55% of 4π		

Table 2
Number of observed events as a function of total centre of mass energy and of event type.

Total centre of mass energy	Number of events	Integral luminosity
3.60 GeV	8	182 nb^{-1}
3.68 GeV (ψ')	117	1119 nb^{-1}
4.17 GeV	18	255 nb^{-1}
4.26 GeV	43	425 nb^{-1}
4.40 GeV	113	1168 nb^{-1}

Event type	Number of events
e + x	170
μ + x	89
e + e	12
$\mu + \mu$	5
e + μ	23

Data have been taken at five different centre of mass energies between 3.60 and 4.40 GeV (see table 2). Events of type (3) were selected by the following criteria:

There are two tracks observed within the internal detector.

In order to suppress various types of QED background such as $e^+e^- \to e^+e^-(\mu^+\mu^-)\gamma$, $e^+e^- \to e^+e^-(\mu^+\mu^-)\gamma\gamma$ and $e^+e^- \to e^+e^-\mu^+\mu^-$, we require the azimuthal angle between the two tracks to be less than 163° in case of events with an identified muon and less than 146° in all other cases. Furthermore, the total measured energy has to be less than 60% of the total centre of mass energy.

No other charged particle or photon is detected within 96% of the full solid angle.

Both tracks must be in the restricted range of the polar angle: $38° < \theta < 142°$. This cut reduces the background from beam–gas reactions which tend to produce particles at small angles with respect to the beam direction.

Each track must have a measured energy of at least 10 MeV in the lead glass counters. Events involving slow protons from beam gas reactions are rejected by this cut.

One of the tracks must have the signature of a muon or an electron: the muon signature is defined by hits in the drift chambers behind the iron absorber; the electron signature is defined by an energy of more than 0.5 GeV measured in the NaI and lead glass counters in the angular range $61° < \theta < 119°$; this restricted angular range is chosen to avoid energy losses due to leakage from the edges of the NaI and lead glass counters. Events with an electron or muon candidate will be referred to as "electron events" or "muon events" respectively. The samples of electron and muon events are not disjoint, but the overlap is small (see table 2).

The coordinate of the event vertex in the beam direction must agree with the nominal interaction point to within 4 cm. Fig. 2 shows the distribution of this coordinate, with the cut indicated, for electron and muon events separately.

In total, there are 299 events observed which fulfil the selection criteria. Table 2 shows how these events are distributed as a function of the centre of mass energy and the type of identified lepton. Particles denoted by X include nonidentified electrons and muons as well as pions and kaons from τ-decays. It should be noted that τ-pair production at 3.68 GeV is enhanced by the vacuum polarization due to the ψ'-resonance. Muon pair production is increased by the same ratio and this latter reaction has been used to determine the en-

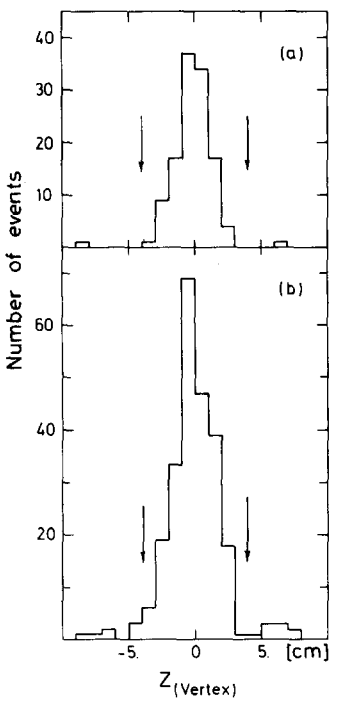

Fig. 2. Distribution of the reconstructed interaction point in the direction of the beam line for muon events (a) and electron events (b).

hancement factor, which we find to be 2.30 ± 0.13.

Various background processes have been considered which might survive the selection criteria and simulate τ-pair production. It should be emphasized that the types of background processes are quite different for electron and muon events, and that these events have been analyzed separately:

The largest part of the background is due to beam gas interactions. It amounts to 6% for electron events and 2% for muon events, averaging over all centre of mass energies. These values have been determined from the vertex distributions along the beam axis (see fig. 2).

The QED reactions $e^+e^- \to \mu^+\mu^-\gamma\gamma$ and $e^+e^- \to \mu^+\mu^-e^+e^-$ can contribute to the muon events. Calculations by Gutbrod and Rek [5] show that for our set of cuts this type of background contributes less than 1% to the signal. The QED reaction $e^+e^- \to e^+e^-\gamma\gamma$, which can contribute to the electron events, is essentially excluded by the wider acoplanarity cut for events without an identified muon candidate.

Various decays [6] of charmed particles might simulate τ-decays, however, less than 1% of the data above the charm threshold can be due to these types of processes. It should be emphasized that the events produced at 3.60 and 3.68 GeV centre of mass energy cannot be due to charm because the energy is below charm threshold.

Background from multihadronic events with two observed tracks and an escaping K_L^0 or neutron can simulate an electron event, if a photon or π^0 is emitted in the direction of one of the charged particles. The rates of these types of background processes have been determined from the angular distribution of identified two prong, one gamma (π^0) events. They amount to less than 1% of the signal.

The total background in the final sample amounts to about 6% for electron events and 2% for muon events. It is not taken into account in the further analysis because it is small as compared to statistical errors.

The energy spectrum of identified electrons is plotted in fig. 3 for the ψ' data (a) and for the 4 GeV region data (b). The full and dashed curves show the behavior of the spectrum as expected from (V − A)- and (V + A)-coupling at the τ-vertex using a mass of about 1.8 GeV. Here and in all further calculations we assume a massless τ-neutrino. Both the (V − A)- and the (V + A)-spectrum are in agreement with the data and reproduce the change with the centre of mass energy.

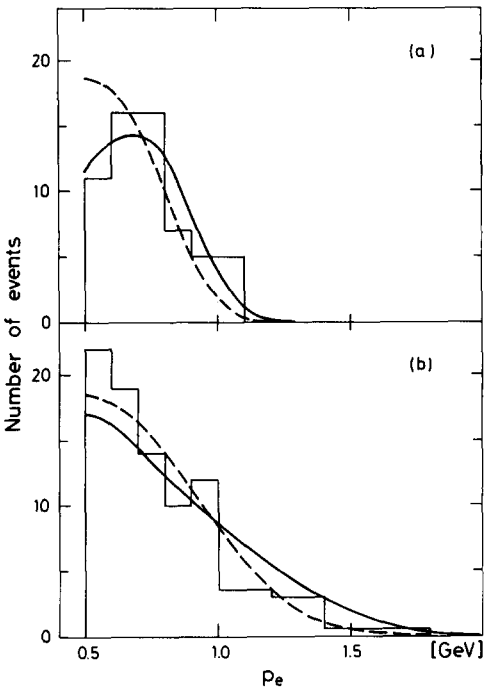

Fig. 3. Energy spectrum of identified electrons from τ-decays using the data taken at 3.68 GeV (a) and above 4 GeV (b) total centre of mass energy. The full and dashed curves show the energy spectrum expected from τ-decays under the assumption of (V − A) and (V + A) coupling, respectively.

In fig. 4 we plot the visible cross section for electron events (full circles) and muon events (open circles) separately as a function of the total centre of mass energy. The double counting of events occurring in the case of e–e, e–μ and μ–μ events is taken into account in the

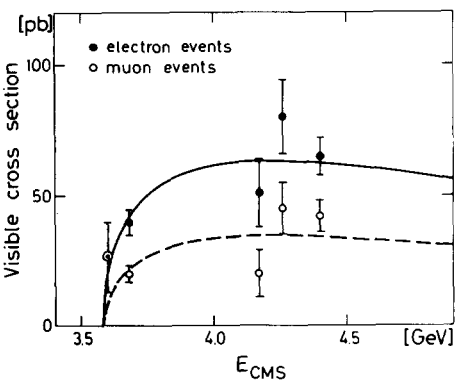

Fig. 4. Visible cross section of electron events and muon events as a function of the total centre of mass energy. The full and dashed curves show the τ-pair production cross section fitted to the data points for electron and muon events, respectively.

acceptance calculations. The acceptance α of the apparatus for the τ-decays listed above under reaction (4) has been calculated with Monte Carlo methods assuming V – A coupling at the τ-vertex and using branching ratios B in the proportions $B_e : B_\mu : (B_\pi + B_K) = 1 : 1 : 0.5$. Pions or kaons from τ-decays might simulate muons by punch through or electrons by interaction in the NaI or lead glass counters. It has been verified that these effects as well as a change of the assumed pion and kaon branching ratio from $(B_\pi + B_K) = 0$ to $(B_\pi + B_K) = B_e$ do not significantly affect the energy dependence of the acceptance. We can, therefore, obtain a value for the mass of the τ-particle by fitting the data with a curve in the shape of the pair-production cross section for pointlike spin-1/2 fermions:

$$\sigma_{vis}(e/\mu) = \sigma_\mu \cdot (1+\delta) \cdot \tfrac{1}{2}\beta \cdot (3-\beta^2) \cdot B_{e/\mu} \cdot B_{1\,prong} \cdot \alpha,$$

where β is the velocity of the τ-lepton in the laboratory system and σ_μ is the cross section for muon pair production. δ is the radiative correction to τ pair production [‡1]. $B_{e/\mu}$ and $B_{1\,prong}$ are respectively the branching ratios for τ-decay into electron (or muon) plus neutrinos and one prong plus neutrino(s). In the fit procedure, the τ-mass and the absolute normalizations of the cross sections are used as free parameters. The fitted curves to electron and muon events are also shown in fig. 4.

As a check we have also determined the τ mass from the electron and muon events separately. The agreement is good. Furthermore the assumption of (V + A) instead of (V – A) coupling has a small effect on the mass parameter. All these results are summarized in table 3. The absolute normalizations from the (V – A) fit are $B_e \cdot B_{1\,prong} = 0.064 \pm 0.005$ and $B_\mu \times B_{1\,prong} = 0.042 \pm 0.005$, where the errors given are statistical only. These numbers are in approximate agreement with the hypothesis $B_e = B_\mu \approx 0.15$ and $B_\pi/B_e = 0.5$. No further conclusion should be drawn, since the systematic errors have not yet been accurately evaluated. It has, however, been verified that under pessimistic assumptions the systematic effects do not significantly change the mass value derived from the fit, because these effects mainly involve particle misidentification, and as mentioned above do not alter the shape of the measured cross section as a function of energy.

In order to obtain a mass value that is independent of the assumed coupling at the τ-vertex, the masses corresponding to the (V – A) and (V + A) hypotheses have been averaged, and the errors have been chosen so that they cover the full error range of both mass values. This yields

$$m_\tau = 1.787^{+0.010}_{-0.018}\ \text{GeV}.$$

This mass value is considerably lower than most previous results [2] but in good agreement with a recent measurement by the DASP-collaboration [3]. This latter result was obtained assuming (V – A) coupling at the τ-vertex.

[‡1] Radiative corrections to τ pair production have been evaluated with a modified version of a computer program developed by Berends et al., for calculating radiative corrections to the process $e^+e^- \to \mu^+\mu^-$ [7]. δ amounts to –0.18 at 14 MeV above the τ production threshold and to –0.12 for the non-resonant contribution at the ψ'-resonance. It decreases rapidly in magnitude with increasing centre of mass energy. The authors wish to acknowledge a helpful discussion concerning the radiative corrections problem with Dr. R. Gastmans of the University of Leuven.

Table 3
Fit results.

	(V – A)			(V + A)		
	M_τ (GeV)	χ^2	degrees of freedom	M_τ (GeV)	χ^2	degrees of freedom
e-events	$1.790^{+0.008}_{-0.012}$	2.5	3	$1.787^{+0.010}_{-0.014}$	2.3	3
μ-events	$1.789^{+0.010}_{-0.019}$	6.3	3	$1.771^{+0.021}_{-0.037}$	5.3	3
all events	$1.790^{+0.007}_{-0.010}$	8.9	7	$1.783^{+0.010}_{-0.014}$	8.0	7

Dr. B. Granz and Mr. P. Lennert contributed substantially to this experiment by their work on the design and construction of the muon chambers. The excellent and efficient work of the DORIS machine group, of the DESY Hallendienst and of the Heidelberg Physics Institute Workshop is gratefully acknowledged. We thank K. Bruder, H. Matsumura and H.J. Seidel for their competent technical assistance and for their help in running the experiment. Furthermore, the members of the Heidelberg group thank the DESY directorate for their kind hospitality. This work was partly supported by the Bundesministerium für Forschung und Technologie.

References

[1] M.L. Perl et al., Phys. Rev. Lett. 35 (1975) 1489.
[2] A summary of experimental results can be found in M.L. Perl's review of heavy lepton production in: Proc. 1977 Intern. Symp. on Lepton and photon interactions at high energies (Hamburg, 1977) p. 145.
[3] DASP Collaboration, R. Brandelik et al., Phys. Lett. 73B (1977) 109.
[4] W. Bartel et al., Phys. Lett. 66B (1976) 483.
[5] F. Gutbrod and Z.J. Rek, DESY Report 77/45 (1977), and private communication.
[6] A. Barbaro-Galtieri, in: Proc. 1977 Intern. Symp. on Lepton and photon interactions at high energies (Hamburg, 1977) p. 21.
[7] Berends et al., Nucl. Phys. B57 (1973) 381; B63 (1973) 381.